Chemical Engineering Journal 116 (2006) 173–178

Chemical Engineering Journal

www.elsevier.com/locate/cej

Catalytic incineration of ethylene oxide in the packed bed reactor

Zorana Lj. Arsenijević [a,*], Boško V. Grbić [a], Nenad D. Radić [a], Željko B. Grbavčić [b]

[a] *Institute for Chemistry, Technology and Metallurgy, Department of Catalysis and Chemical Engineering, Njegoseva 12, Belgrade, Serbia and Montenegro*
[b] *Faculty of Technology and Metallurgy, University of Belgrade, Karnegijeva 4, Belgrade, Serbia and Montenegro*

Received 19 April 2005; received in revised form 21 November 2005; accepted 23 November 2005

Abstract

Investigations of catalytic incineration of ethylene oxide (ETO) over Pt/Al_2O_3 catalyst have been conducted on laboratory and pilot scale level. The measurements of the reaction rate conducted under gradientless conditions have been used to evaluate kinetics parameters valuable for reactor modeling. A reactor model is proposed which could a priori predict behavior of catalytic convertor under various operating conditions (inlet temperature, inlet pollutant concentration and space velocity) based on the kinetics parameters and mass and energy balances. The results show satisfactory agreement between predicted and experimental values of conversion and temperature profiles along the catalyst bed.
© 2005 Elsevier B.V. All rights reserved.

Keywords: Pt/Al_2O_3 catalyst; Ethylene oxide; Catalytic oxidation; Kinetics; Reactor model

1. Introduction

Ethylene oxide (ETO) emission from numerous stationary sources such as ETO production plants, manufacture of ethylene glycol, polymers, surfactants, etc., is considered as very important due to environmental risks [1]. Besides, significant quantity of ETO is released to the atmosphere from sterilization processes of health-care materials and other heat-sensitive products in medical facilities. The ETO concentration in the exhausted gases substantially depends on the sort of stationary source. Generally, ETO production plants (partial oxidation of ethylene over Ag catalysts) are expected to release low concentration of ETO in waste gases, along with ethane and ethylene. Estimated emission of ETO from production plants are in the range 1.0–0.5 kg/t_{ETO} [1]. On the other hand, ETO emission from sterilizing units can vary from 0.1 to 90 vol.%, depending on the stage of the sterilizing process.

Due to its high degradability, ETO is not expected to contribute to the formation of ground-level ozone or to the depletion of the stratospheric ozone layer. In addition, its contribution to the greenhouse effect is considered to be negligible [2]. Mostly ETO is released to the atmosphere, and little transfer to water or soil is expected. Therefore, the potential for adverse effects is greatest for organisms exposed to contaminated air. An effect of ETO on human health consists of inducing a wide range of tumors and interactions with genetic material. Generally, it is considered that exposure to ETO at any level is harmful to health. For these reasons, based on the present air quality regulations in effect, during the emission of ETO at a mass flow of 25 g/h or more a mass concentration of 5 mg/m^3 in the exhaust gas, corresponding to 2.8 ppm, may not be surpassed.

Different technologies can be used to treat ETO emissions: wet-scrubbers, thermal oxidizers, catalytic oxidizers and reactors or columns loaded with solid sorbents (so-called "dry-bed" reactors). Wet-scrubbers absorbs ETO into a recirculating water–acid solution, converting ETO to ethylene glycol. When the acid solution becomes saturated with ethylene glycol, it is transferred into a waste treatment device. Thermal oxidizers operate by oxidizing or burning ETO to form the products of carbon dioxide, water vapor and heat. Thermal oxidizers generally require additional fuel. Catalytic oxidizers operate with the same end result as the thermal oxidizers but at lower temperatures. "Dry-bed" reactors eliminate ETO by causing it to bind permanently to the solid reactant. They operate at an ambient temperature.

The appropriateness of the previous technologies for the specific process depends on several factors such as: efficiency, energy consumption, secondary pollution, capital investments, etc. The principal advantages of catalytic oxidation are high efficiency of the process, low energy consumption and absence of

* Corresponding author. Tel.: +381 11 3370408; fax: +381 11 3370500.
E-mail address: zorana@elab.tmf.bg.ac.yu (Z.Lj. Arsenijević).

1385-8947/$ – see front matter © 2005 Elsevier B.V. All rights reserved.
doi:10.1016/j.cej.2005.11.007

Nomenclature

A	pre-exponential factor (kg/kg$_{cat}$ s)
a_p	outer surface area of the particles per unit volume (m^2/m^3)
C	reactant concentration (vol.%)
C_p	fluid heat capacity (kJ/kg °C)
D_c	reactor (bed) diameter (m)
D	diffusivity of ETO in air (m^2/s)
d_p	particle diameter (m)
E	activation energy (kJ/mol)
H	bed height (m)
ΔH_r	heat of reaction (kJ/kg)
h_p	heat transfer coefficient (kW/m^2 °C)
j_D	mass transfer factor
j_H	heat transfer factor
k	rate constant (kg$_{ETO+air}$/kg$_{cat}$ s)
k_m	mass transfer coefficient (m/s)
Nu_p	Nusselt number ($=h_p d_p/\lambda$)
Pr	Prandtl number ($=\mu C_p/\lambda$)
R	correlation factor, in Fig. 2.
Re_p	particle Reynolds number ($=d_p \rho_f U/\mu$)
r	reaction rate (m^3 vol.%/kg$_{cat}$ s), in Eq. (1)
r_A	reaction rate (kg/kg$_{cat}$ s)
Sc	Schmidt number ($=\mu \rho_f/D$)
Sh_p	Sherwood number ($=k_m d_p/D$)
SV	space velocity (h^{-1})
T_f	fluid temperature (°C)
T_p	catalyst temperature (°C)
U	superficial fluid velocity [$=V/(\pi D_c^2/4)$] (m/s)
V	volumetric fluid flowrate (m^3/s)
W_f	mass flux of gas phase (kg/m^2 s)
x_A	conversion
y	mass fraction of the reactant in the fluid (kg/kg)
y_p	mass fraction of the reactant in the fluid just above catalyst surface (kg/kg)
z	vertical coordinate (m)

Greek symbols

ε_a	bed voidage
μ	viscosity of the fluid (N s/m^2)
λ	thermal conductivity of the gas (kW/m °C)
ρ_f	fluid density (kg/m^3)
ρ_p	particle density (kg/m^3)

Subscripts

0	at the bed inlet ($z=0$)
H	at the top of the bed ($z=H$)

secondary pollution (NO_x or liquid or solid waste). The supported noble catalysts are widely used for catalytic oxidation of organic vapors, particularly platinum, because of its high selectivity, resistance to poisoning and low ignition temperature. A preheater must be used to bring the inlet gases to the appropriate initiation reaction temperature.

The purpose of this work was to develop a reactor model for predicting the catalytic incineration of ETO over sphere shaped Pt/Al_2O_3 catalyst under various operating conditions (inlet temperature, inlet concentration and space velocity). Since there are no available literature data on the kinetics and the mechanism of ETO oxidation over Pt/Al_2O_3 catalyst, kinetics of this process was investigated in order to evaluate parameters useful for modeling and design of catalytic ETO incinerator.

2. Experimental

2.1. Catalyst

A Pt/Al_2O_3 catalyst was prepared by dry impregnation of sphere shaped Al_2O_3 support (Rhone Poulenc) with aqueous solution of platinum precursor [3]. Detailed procedures of catalyst preparation, subsequent processing and characterization is presented elsewhere [4]. Key features of the catalyst are summarized in Table 1.

2.2. Kinetic investigations

The experiments were performed in an external recycle reactor designed for reaction kinetic studies. The apparatus and the method of measuring the rate of ETO oxidation were described in Radic et al. [5]. The inlet and the outlet concentrations of ETO was analyzed by an FID detector using stainless-steel column, 6.5 ft long and 1/8 in. in diameter, containing 1% SP-1000 carbopack B. Oxygen was analyzed using a 2 m column with molecular sieve 13X, and a TCD detector. The measurements were performed under gradientless conditions, feed flow rate was 10 l/h and the recirculation flow rate was kept on 1300 l/h. At the constant feed flow rate of 10 l/h the change of overall recycle flow rate from 500 to 1300 l/h at temperatures up to 142 °C had no influence on the conversion of ETO. This implies that recycle flow rate of 500 l/h was sufficient to eliminate almost any mass and temperature transfers effects on overall conversion measured. The recycle flow rate of 1300 l/h was chosen because it allowed maintaining stable reaction conditions. Also, this flow significantly exceeds recycling ratio of 25 that is required to allow assumption for gradientless conditions [6]. The reproducibility of the results was verified by carrying out each test several times. The kinetics measurements were performed at ETO conversion below 20%.

Besides, short test have been conducted with glass spheres instead Pt catalyst in the investigated temperature range of 150–200 °C. The ETO conversion was not observed in these tests.

Table 1
Catalyst characteristics

Mean diameter (mm)	3.3	Porosity (%)	66
Surface area (m^2/g)	96	Pt loading (wt.%)	0.12
Density (kg/m^3)	3329	Pt dispersion (%)	86
Apparent density (kg/m^3)	1300	Pt distribution	Egg shell
Pore volume (m^3/kg)	0.58	Width of Pt band (μm)	∼100

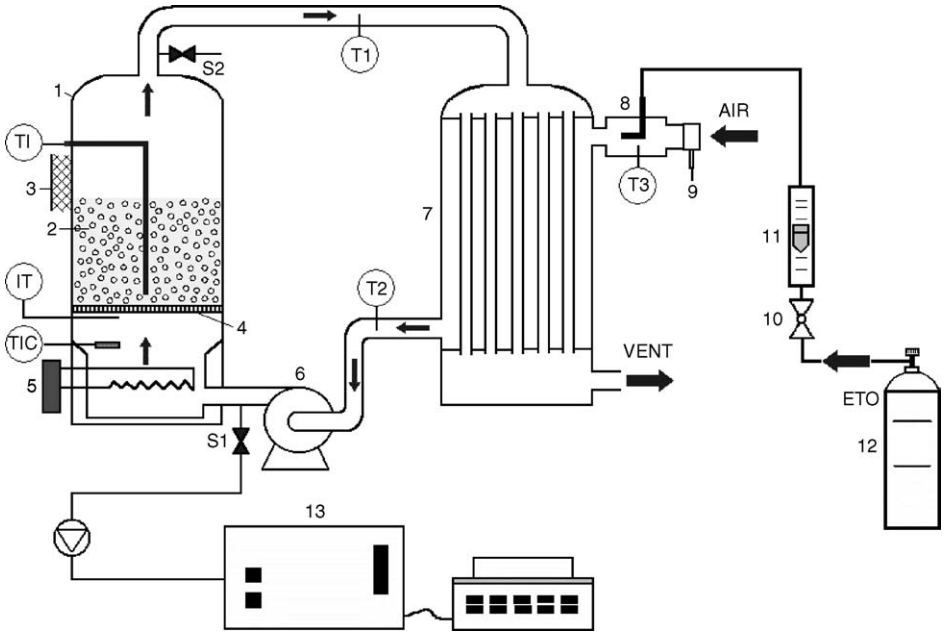

Fig. 1. Pilot scale unit: (1) column; (2) Pt/Al_2O_3 catalyst; (3) thermoisolation; (4) gas distributor; (5) heater; (6) blower; (7) heat exchanger; (8) reaction mixture feeding system; (9) anemometer; (10) valve for ETO flow rate regulation; (11) flowmeter; (12) ETO supply cylinder; (S1,S2) needle valves for gas sampling; (TIC) temperature controller; (IT) inlet temperature indicator; (TI) movable NiCr–Ni thermocouple; (T1/T3) NiCr–Ni thermocouples; (13) gas chromatograph.

The reaction rate was calculated by the following equation:

$$r = \frac{F}{W}(C_0 - C) \tag{1}$$

where F is feed flow rate (m^3/s), W is catalyst weight (kg), C_0 is ETO inlet (vol.%) and C is ETO outlet concentration (vol.%).

The investigations were performed in the 67–142 °C temperature range, and the ETO concentrations in air varied up to 1 vol.%.

2.3. Pilot unit

A schematic diagram of the pilot scale unit is shown in Fig. 1. The unit is designed in order to test wide range of pollutants under real industrial conditions. The unit consists of stainless-steel reactor 315 mm in diameter (1) loaded with catalyst (2), heat exchanger (7), blower (6), electrical air preheater with temperature control unit (5) and system for ETO vapor introduction (8). Concentration of ETO at the inlet and at the outlet was measured by on-line gas chromatograph equipped with flame ionization detector (FID). Temperature was continuously recorded at the all characteristic points of the unit, as indicated in Fig. 1. Axial temperature profile through the bed was measured by movable thermocouple (TI).

The ranges of operating conditions were the following: space velocity 7800–25 100 h^{-1}, inlet temperature 130–240 °C and ETO inlet concentration 0.02–0.65 vol.%.

2.4. Reactor model

The one-dimensional reactor model neglecting limitations of internal pore diffusion can be formulated considering mass and energy balance over an increment of the adiabatic catalyst bed.

Mass balance

Reactant consumed at the catalyst surface due to the chemical reaction:

$$W_f \frac{dy}{dz} = (1 - \varepsilon_a)\rho_p r_A = (1 - \varepsilon_a)\rho_p k y_p \tag{2}$$

Reactant transferred from the bulk flow to the catalyst surface:

$$W_f \frac{dy}{dz} = k_m a_p \rho_f (y - y_p) \tag{3}$$

Energy balance

Heat generated in the solid phase due to the chemical reaction:

$$W_f C_p \frac{dT_f}{dz} = (1-\varepsilon_a)\rho_p(-\Delta H_r)r_A = (1-\varepsilon_a)\rho_p(-\Delta H_r)k y_p \tag{4}$$

Heat transferred from the catalyst into the gas phase:

$$W_f C_p \frac{dT_f}{dz} = h_p a_p (T_p - T_f) \tag{5}$$

where a_p represents outer surface area of the particles per unit bed volume:

$$a_p = \frac{6(1 - \varepsilon_a)}{d_p} \tag{6}$$

By combining Eqs. (2) and (3) the ratio (mass fraction of the reactant in the fluid just above catalyst surface)/(mass fraction of the reactant in the bulk flow) is:

$$\frac{y_p}{y} = \frac{1}{1 + k\rho_p d_p / 6 k_m \rho_f} \tag{7}$$

Note that for $y_p/y \to 1$ the overall process is controlled by the reaction kinetics, while for $y_p/y \to 0$ the overall process is controlled by the mass transfer.

Heat and mass transfer coefficients were evaluated using Handley and Heggs [7] correlation:

$$j_H = j_D = \frac{0.255}{\varepsilon_a Re_p^{1/3}} \quad (8)$$

where

$$Nu_p = \frac{h_p d_p}{\lambda} = j_H Re_p Pr^{1/3} \quad (9)$$

and

$$Sh_p = \frac{k_m d_p}{D} = j_D Re_p Sc^{1/3} \quad (10)$$

The packed bed heat transfer correlation of Handley and Heggs [7] has been recommended by several sources for $Re_p < 500$ [8–10]. For mass transfer, the same correlation may be used by substituting Sh_p and Sc for Nu_p and Pr [10].

Obtained parameters from kinetic measurements were included into the model described above in order to a priori predicting reactor performance, i.e. variation of conversion, bulk reactant concentration, surface reactant concentration, fluid temperature and particle temperature with bed height. Eqs. (2)–(10) are solved using standard numerical procedure. The initial conditions are as follows: $y = y_0$, $T_f = T_{f0}$ and $T_p = T_{p0} = T_{f0}$ at $z = 0$.

Having in mind the low ETO concentration, physical characteristics of reacting mixture at a given temperature were calculated assuming that reaction mixture is pure air.

The model had used ETO heat of combustion, $\Delta H_{r(25\,^\circ C)} = 1306.04 \times 10^3$ kJ/kmol [11] and ETO diffusion coefficient in air $D_{air+ETO(0\,^\circ C)} = 0.1355 \times 10^{-4}$ m^2/s calculated according to empirical corelations [12].

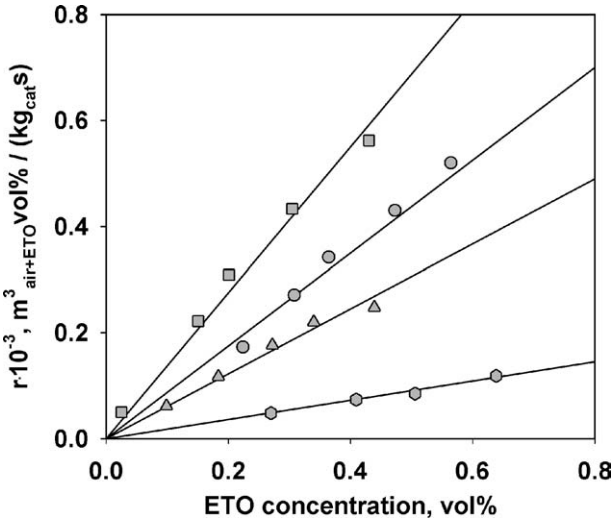

Fig. 2. Reaction rate vs. ETO concentration.

3. Results and discussion

3.1. Kinetics investigations

Having in mind ETO lower explosion limit of 2.7 vol.%, the range of investigated ETO concentrations have been confined up to the 1.0 vol.%.

Dependence of ETO oxidation rate versus ETO concentration is presented in Fig. 2.

There is a linear dependence of the reaction rate on ETO concentration over entire concentration range (Fig. 2) indicating that reaction rate is the first order with respect to ETO.

Since the molar ratio O_2/ETO was in the range from 20 to 1000, oxygen concentration on the catalyst surface is assumed relatively high. Therefore, zero reaction order with respect to oxygen was considered.

The first order of ETO oxidation kinetics could be described by several kinetics mechanisms; the Langmuir–Hinshelwood

Table 2
Comparison of experimental data with model predictions

Run	H (cm)	V_0 (m^3/h)	SV (h^{-1})	C_0 (vol.%)	T_{f0} (°C)	$T_{fH,exp}$ (°C)	$T_{fH,cal}$ (°C)	$x_{A,exp}$ (%)	$x_{A,cal}$ (%)
1	15.00	103.1	8096	0.8302	233	555	587.4	99.87	100.00
2	15.00	163.6	12853	0.2744	118	120	156.0	34.24	30.54
3	15.00	152.9	12012	0.2940	139	208	247.5	84.50	82.26
4	15.00	131.5	10330	0.3430	182	309	333.2	99.30	99.99
5	15.00	151.4	11892	0.0798	190	214	222.1	99.70	90.32
6	15.00	250.8	19699	0.4410	191	328	384.1	99.50	99.96
7	9.25	141.6	16942	0.2324	193	275	292.2	89.90	96.91
8	9.25	138.1	16514	0.2464	240	334	347.3	97.40	99.90
9	9.25	146.3	17501	0.2296	183	265	277.0	87.14	92.59
10	9.25	156.4	18709	0.2184	131	154	156.5	31.70	25.62
11	9.25	155.7	18621	0.2156	153	209	203.1	38.50	51.82
12	6.75	105.5	16827	0.4970	191	373	407.2	96.03	99.72
13	6.75	131.5	20973	0.5936	191	429	448.9	97.40	99.97
14	6.75	137.9	22000	0.5488	190	409	429.0	92.70	99.80
15	6.75	133.0	21214	0.5628	199	421	443.7	97.40	99.91
16	5.00	111.6	26142	0.5656	190	409	435.5	90.50	99.48
17	5.00	102.1	23922	0.5782	200	442	451.0	93.24	99.77

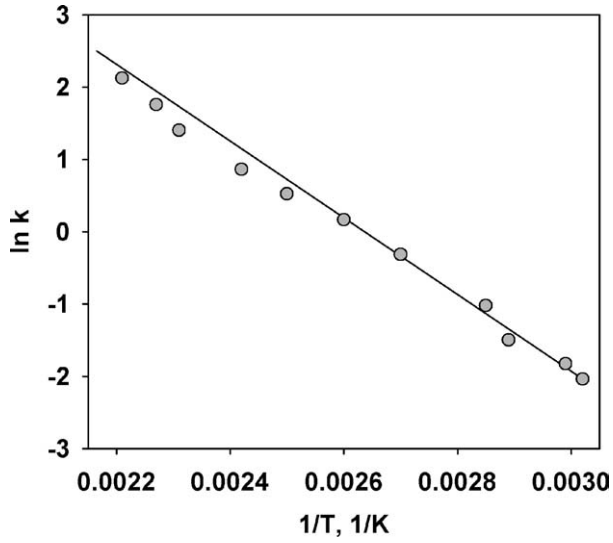

Fig. 3. Arrhenius plot for ETO oxidation.

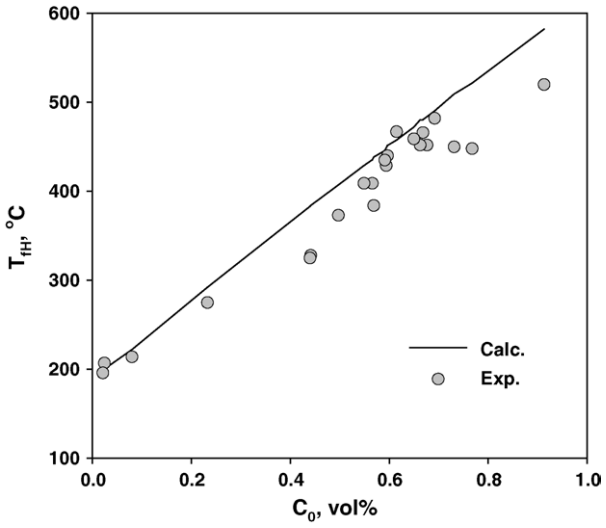

Fig. 5. Maximum catalyst temperatures vs. inlet ETO concentration (T_{f0} = 190 °C).

mechanism where surface reaction proceeds between weakly adsorbed species; the Eley–Rideal mechanism where the surface oxygen reacts with ETO from a gas phase. Also, the Mars–van Krevelen kinetic model, that has received a wide support in literature [13–15] for the hydrocarbon oxidation over noble metal catalysts, could describe reaction as interaction between ETO with oxidized surface. Kinetics results do not provide deeper insight into the reaction mechanism and further comprehensive investigations are required.

The temperature dependence of the rate constants (k), calculated on the basis of simple power law equation, determined reaction order and reaction rate, is presented on an Arrhenius plot in Fig. 3. The slope gives activation energy value of 42 ± 2 kJ/mol and the intercept on ordinate gives the pre-exponential factor value of 585 ± 15 $kg_{air+ETO}/(kg_{cat}\ s)$. These values were used in model calculations.

3.2. Model testing

Comparison between the experimental and calculated values for converter efficiency and outlet catalyst temperature along with the inlet conditions is presented in Table 2, for some runs.

The results from the Table 2 indicate satisfactory agreement between calculated and experimental results for ETO conversion and catalyst outlet temperatures. In addition, there are some disagreements for converter efficiency between model and experimental data in the range of lower inlet temperatures. In order to illustrate the model validity for prediction of ETO conversions with inlet gas temperatures for space velocity of 16 000–19 800 h^{-1} and inlet ETO concentration in range of 0.21–0.65 vol.% is shown in Fig. 4. Fig. 5 presents agreement between predicted and experimental data for outlet temperatures from the catalyst bed for approximately constant inlet gas

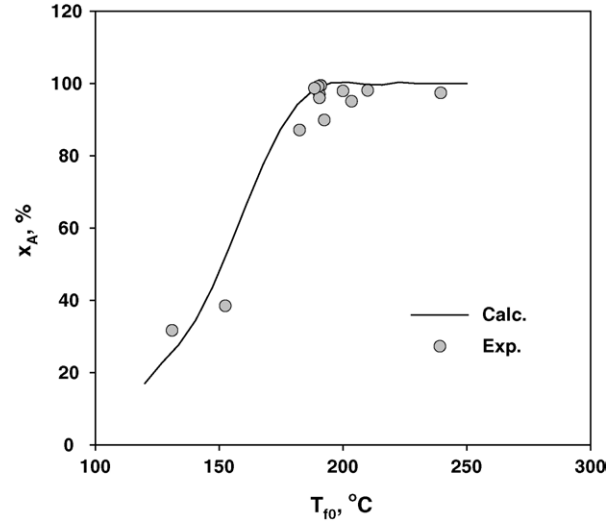

Fig. 4. ETO conversions vs. inlet gas temperatures (SV = 16 000–19 800 s^{-1}, C_0 = 0.21–0.65 vol.%).

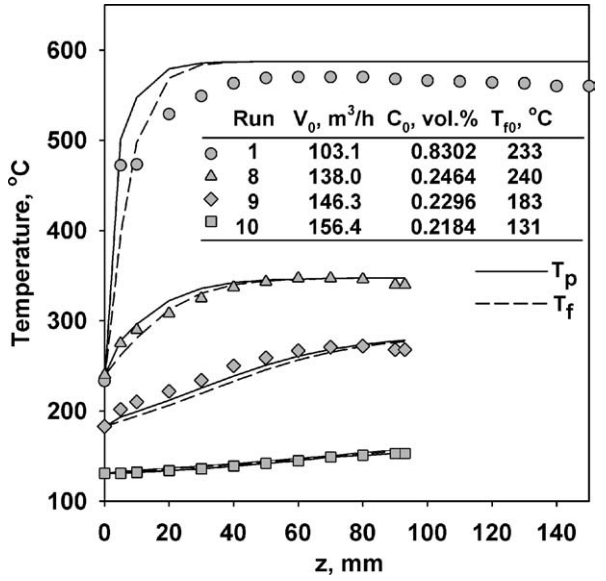

Fig. 6. Temperature profiles along the catalyst bed.

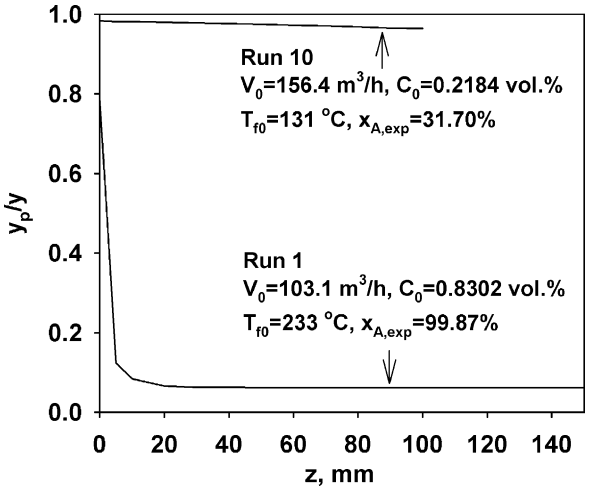

Fig. 7. Ratio y_p/y vs. catalyst bed height.

temperature of 190 °C. As can be seen from Fig. 5, calculated maximum temperatures slightly overpredict measured temperatures at the outlet of the catalyst bed, probably due to certain heat losses.

Beside the prediction of catalyst outlet temperature, the reactor model also enables the prediction of temperature profiles along the catalyst bed. This is presented in Fig. 6 for four typical runs (runs 1, 8, 9 and 10).

Furthermore, the reactor model can illustrate reaction regimes along the catalyst bed height by means of ratio y_p/y. The computed axial values of y_p/y for the runs 1 and 10 are presented in Fig. 7. The low conversion curve (run 10) shows that the ratio y_p/y only slightly differs from 1 through the entire catalyst bed indicating that the process is controlled by kinetics of surface reaction. The sharp drop of ratio y_p/y for the high conversion curve (run 1) point out that intrinsic kinetics prevails only within very narrow inlet catalyst section. Through the rest of the catalyst bed, external mass transfer governs the overall process.

4. Conclusions

The measurements of the reaction rate conducted under gradientless conditions have shown that ETO deep oxidation in the air can be presented by first order kinetics with respect to ETO and pre-exponential factor A of $585 \pm 15\ kg_{air+ETO}/(kg_{cat}\ s)$ and activation energy E of 42 ± 2 kJ/mol were determined.

These kinetic parameters of ETO oxidation over Pt/Al_2O_3 catalyst combined with a mass and energy balances into reactor model successfully simulate the catalytic incinerator operation. The agreement between calculated and experimental data obtained on pilot scale unit confirms the model validity.

Acknowledgement

This study was supported by the Ministry for Science, Technology and Development, Republic of Serbia.

References

[1] O. Rentz, Emissions of Volatile Organic Compounds (VOC) from Stationary Sources and Possibilities of their Control, ECE VOC Task Force Report (91-010), Karlsruhe, 1990.
[2] Assessment Report—Ethylene oxide, Canada Gazette Part 1, vol. 136, no. 15, 2002, pp. 193–195 (http://canadagazette.gc.ca/archives-e.html).
[3] B. Grbic, V. Dondur, D. Jovanovic, A. Terlecki-Baricevic, The effect of Pt location in Pt/Al_2O_3 catalyst on its oxido-reducing activity and resistance to SO_2 poisoning, J. Serb. Chem. Soc. 58 (12) (1993) 1071–1079.
[4] B. Grbic, N. Radic, A. Terlecki-Baricevic, Crystallite size effects on kinetics of toluene oxidation on Pt/Al_2O_3 catalysts, Sci. Sinter. 30 (3) (1998) 179–189.
[5] N. Radic, B. Grbic, A. Terlecki-Baricevic, Kinetics of deep oxidation of *n*-hexane and toluene over Pt/Al_2O_3 catalysts. Platinum crystallite size effect, Appl. Catal. B: Environ. 50 (2004) 153–159.
[6] J.M. Berty, Testing commercial catalysts in recycle reactors, Catal. Rev. Sci. Eng. 20 (1) (1979) 75–96.
[7] D. Handley, P.J. Heggs, Momentum and heat transfer mechanism in regularly shaped packing, Trans. Inst. Chem. Eng. 46 (1968) T251–T264.
[8] G.F. Froment, K.B. Bischoff, in: G.F. Froment, K.B. Bischoff (Eds.), Chemical Reactor Analysis and Design, Wiley, New York, 1978 (Chapters 3 and 11).
[9] F. Krieth, W.Z. Black, in: F. Krieth, W.Z. Black (Eds.), Basic Heat Transfer, Harper & Row, New York, 1978 (Chapters 3 and 11).
[10] B. Hook, H. Littman, M.H. Morgan III, Y. Arkun, A priori modeling of an adiabatic spouted bed catalytic reactor, Can. J. Chem. Eng. 70 (1992) 966–982.
[11] EPA-450/4-84-007L, Locating and estimating air emissions from sources of ethylene oxide, U.S. Environmental Protection Agency, Office of Air and Radiation, Office of Air Quality Planning and Standards, Research Triangle Park, North Carolina 27711, Report No. EPA-450/4-84-007L, 1986.
[12] R.C. Reid, J.M. Prausnitz, T.K. Sherwood, Diffusion coefficients, in: R.C. Reid, J.M. Prausnitz, T.K. Sherwood (Eds.), The Properties of Gases and Liquids, McGraw-Hill, New York, 1977, p. 554.
[13] S. Gangwal, K. Ramanathan, P. Caffrey, M. Mullins, J. Spivey, Mixture effects in the catalytic oxidation of VOCs in air, U.S. Environmental Protection Agency, Research Triangle Park, North Carolina, Report No. EPA-600/7-88-017, 1988.
[14] S.K. Gangwal, M.E. Mullins, J.J. Spivey, P.R. Caffrey, B.A. Tichenor, Kinetics and selectivity of deep catalytic oxidation of *n*-hexane and benzene, Appl. Catal. 36 (1988) 231–247.
[15] S. Ordonez, L. Bello, H. Sastre, R. Rosal, F.V. Diez, Kinetics of the deep oxidation of benzene, toluene, *n*-hexane and their binary mixtures over a platinum on γ-alumina catalyst, Appl. Catal. B: Environ. 38 (2) (2002) 139–149.